NASA TECHNICAL MEMORANDUM

NASA TM X-52360

NASA TM X-52360

EFFECT OF COMBUSTOR PARAMETERS ON THE STABILITY OF GASEOUS HYDROGEN-LIQUID OXYGEN ENGINE

by C. E. Feiler

Lewis Research Center
Cleveland, Ohio

TECHNICAL PAPER proposed for presentation at Fourth Combustion Conference sponsored by the Interagency Chemical Rocket Propulsion Group
Menlo Park, California, October 2-13, 1967

NATIONAL AERONAUTICS AND SPACE ADMINISTRATION · WASHINGTON, D.C. · 1967

EFFECT OF COMBUSTOR PARAMETERS ON THE STABILITY OF GASEOUS HYDROGEN-LIQUID OXYGEN ENGINE

by C. E. Feiler

Lewis Research Center
Cleveland, Ohio

TECHNICAL PAPER proposed for presentation at

Fourth Combustion Conference
sponsored by the Interagency Chemical Rocket Propulsion Group
Menlo Park, California, October 2-13, 1967

NATIONAL AERONATUICS AND SPACE ADMINISTRATION

EFFECT OF COMBUSTOR PARAMETERS ON THE STABILITY OF GASEOUS HYDROGEN-LIQUID OXYGEN ENGINE

by C. E. Feiler

National Aeronautics and Space Administration
Lewis Research Center
Cleveland, Ohio

E-4207

ABSTRACT

Stability limits from the response factor model have been obtained for variations in chamber pressure, flow rate, throat area, and oscillation frequency for a fixed injector element geometry, and are compared with experimental data. The calculated limits were obtained under the assumption that, except for frequency, these variables would not affect the nozzle or liquid oxygen response factors. The comparison of experiment and analysis showed very good agreement which supports the assumption. For constant operating parameters, the stability limit defined by the hydrogen density at transition exhibited a minimum when plotted against frequency. Thus, at a low enough hydrogen density, instability should not occur at any frequency, while at some higher density, an upper and lower frequency limit is predicted.

INTRODUCTION

The response factor model presented in reference 1 assumes that the stability of an engine is controlled by the dynamic coupling that occurs between chamber pressure oscillations and the various combustion or flow processes. If the total coupling produces a large enough in-phase energy addition, instability will result. For gaseous hydrogen-liquid oxygen engines this coupling has been evaluated in the form of a response factor, a measure of in-phase energy addition, for three processes. These processes are the response of the hydrogen flow (ref. 1) the response of vaporizing liquid oxygen drops (ref. 2), and the response of the nozzle flow (ref. 1).

The present extension of this model was suggested by the data of reference 3. These data show the effect of total flow rate, chamber pressure, and nozzle throat area on hydrogen transition temperature or density. Analytical results of the present study are compared with the experimental data. Analytical results of the effect of frequency on hydrogen transition density were also obtained although no experimental data were available for comparison. Such frequency effects could be produced experimentally by changing the chamber diameter. If this were done while also increasing the number of injector elements and the throat area, the engine thrust would be increased.

ANALYTICAL MODEL

The stability criterion assumed in reference 1 was

$$\Sigma N = \frac{\overline{W}_{lox}}{\overline{W}_t} N_{lox} + \frac{\overline{W}_{H_2}}{\overline{W}_t} N_{H_2} + \frac{\overline{W}_t}{\overline{W}_t} N_{noz} = 0 \qquad (1)$$

where N's are the response factors for the various processes considered. The response factors are weighted by the fraction of the total flow, $\overline{W}i/\overline{W}t$ entering into the particular process, i.

In general, if the chamber pressure and flow rate perturbations, P'_c and W', are given nondimensionally by

$$P'_c = P'_{c,max} \sin \omega t \tag{2}$$

$$W' = W'_{max} \sin (\omega t + \theta) \tag{3}$$

where ω is angular frequency, t is time and θ is a phase angle

then $$N = (W'_{max}/P'_{c,max}) \cos \theta \tag{4}$$

Equations for N_{lox} were derived in reference 2. Figure 1 shows N_{lox} plotted against dimensionless time. As shown, the value of N_{lox} peaks at a particular frequency and then decreases to negative values as frequency is increased further. For the results presented herein, N_{lox} was treated as constant at a value of 0.55, the peak value obtained by linear analysis.

The nozzle response factor was derived in reference 1, which treated the nozzle as a resistive flow device. The value of N_{noz} was 0.833.

Figure 2 shows a sketch of an injector element and the equations entering into the lumped element treatment of the hydrogen flow. Figure 3 shows the resulting equations defining N_{H_2} from reference 1 that were solved for various values of the chamber pressure, flow rate, and frequency.

RESULTS AND DISCUSSION

The hydrogen response factor is plotted against hydrogen injection density in figure 4 for several flow rate-chamber pressure combinations. These curves are for a mixture ratio of 5.5 and an oscillation frequency of 3400 cycles per second. In reference 1, τ_b determined by fitting one set of data was 0.00009 seconds. For the present data, a slightly better fit was obtained by changing τ_b to 0.00008 seconds. It can be seen that as hydrogen density is increased (temperature decreased) that the response factor curves also increase. The rate of increase is more rapid for lower flow rates. A similar effect occurs for the lower chamber pressures.

The value of N_{H_2} needed to satisfy the stability criterion (equation 1) for the values of N_{lox} and N_{noz} previously given is 2.39 at a mixture ratio of 5.5. From figure 4 the density corresponding to this value can be obtained for given conditions. Figures 5, 6, and 7 show the variation of hydrogen transition density so obtained against flow rate (varying nozzle area) at constant chamber pressure, flow rate (varying chamber pressure) at constant throat area, and chamber pressure (varying nozzle area and flow rate) respectively. Also shown on figures 5, 6, and 7 are experimental transition densities from reference 3 that were obtained under conditions nominally equivalent to those used for calculating the analytical curves. The predominant effect among the three variables was associated with flow rate. Thus, in figure 7, several flow rates, corresponding to the experimental data were needed to relate the

analysis and experiment. Over a broad range of chamber pressures, exceeding about 250 psi, transition density is seen to be almost invariant with chamber pressure.

The agreement between experiment and theory as shown by the figures was quite good. It is interesting that this correlation was obtained by treating the oxygen response as invariant over the range of parameters experimentally studied. In general, it might have been expected that over this range, a variation of the oxygen response factor would have been necessary; however it was not. The behavior observed is thus associated with the hydrogen response factor and more particularly, with the resistance terms in the response factor represented by the hydrogen injection pressure drop. Thus, when the pressure drop becomes small enough, the hydrogen flow couples with and drives the chamber pressure oscillations. Since figures 5 and 6 show an almost linear variation of hydrogen transition density with flow rate and since hydrogen injection area was constant, the transition boundary is approximately represented by a constant hydrogen injection velocity as opposed to a constant hydrogen-oxygen velocity ratio. This result suggests that the effect of the oxygen system on stability should be related to the oxygen injector geometry and especially oxygen jet diameter as was proposed in reference 4, as an alternative to oxygen injection velocity.

The effect of oscillation frequency on hydrogen transition density is shown in figure 8 for a fixed injector element and combustor conditions. Curves are shown with the oxygen response factor either constant or varying with frequency. The small difference is due to the small variation that occurs in the oxygen response factor over this frequency range. The primary shape of the curves is associated with the hydrogen response factor. It is seen that the model predicts a hydrogen density below which stability always occurs. At higher densities there are lower and upper frequency limits.

At any density above the lower limit the curves might predict stable operation for the fundamental chamber frequency but predict that instability should occur at some harmonic frequency. Thus, for the experimental data discussed, the fundamental frequency for the tangential mode was 3400 cps and for this frequency and the conditions shown in figure 8 a transition density of 0.505 pounds per cubic foot was predicted. From figure 8, instability in the second transverse mode (5640 cps) would have been expected at a density of about 0.3 pounds per cubic foot. The second tangential mode has not been reported in these experiments so it apparently has not occurred at high amplitudes. Instability in higher harmonic modes has been observed in engines such as the M-1, however.

CONCLUDING REMARKS

The form of the response factor model given in equation 1 is general in nature. Although only three processes have been considered at present, there is no reason other processes could not be included in the model. Thus, for example, a term representing the effect of an acoustic liner could readily be added. The barrier to such addition lies in formulating the response factor for the particular process involved. A complete model might also include representations of the atomization and mixing processes and others.

The model could also be adapted, in principle, to any propellant combination, provided that the processes controlling its combustion were known. Thus, the model for heptane-liquid oxygen propellants might consist of response factors for the vaporization of each propellant and for the nozzle.

SUMMARY OF RESULTS

The response factor model for predicting gaseous hydrogen-liquid oxygen engine stability has been extended to show the effects of combustor parameters and oscillation frequency. The results are:

1. Instability associated with changing flow rate or chamber pressure for fixed injector element geometry was related to the response of the hydrogen flow system. Agreement between experiment and analysis was good when compared under the assumption that only the hydrogen flow system response was a variable.

2. For the oxygen system, oxygen injector configuration (jet diameter) rather than oxygen injection velocity appears to have the chief influence on stability. Oxygen jet diameter appears to be the primary parameter for influencing the oxygen response factor.

3. Frequency analysis showed the existence of an upper and lower frequency limit at higher hydrogen injection densities. At sufficiently low densities, stability was predicted at all frequencies.

4. The frequency analysis also predicts harmonic instability in some cases where fundamental mode instability could not occur. Such behavior has been observed in larger engines.

SYMBOLS

A cross-sectional area

C capacitance, $\bar{\rho}V/\gamma\bar{W}$

g gravitational constant

I inductance, $\bar{W}(L/A_1)/g\bar{P}_2$

N response factor

O/F oxidant-fuel mixture ratio

P pressure

P_d hydrogen dome pressure

P_1 annulus entrance pressure

P_2 orifice entrance pressure

s Laplace operator

t time

V dome volume

W flow rate

γ specific heat ratio

θ phase angle

ρ hydrogen density

τ_b time delay constant for hydrogen response

τ_v drop vaporization time

ω angular frequency

subscripts

lox liquid oxygen

max peak amplitude of sine wave

noz nozzle

1 hydrogen annulus

2 hydrogen orifice

b burned hydrogen gases

c chamber

T nozzle throat

t total

superscripts

- average value

' perturbation quantity, $(\overline{X}-\overline{X})/\overline{X}$

REFERENCES

1. Feiler, Charles E.; and Heidmann, Marcus F.: Dynamic Response of Gaseous-Hydrogen Flow System and Its Application to High-Frequency Combustion Instability. NASA TN D-4040, 1967.

2. Heidmann, Marcus F.; and Wieber, Paul R.: Analysis of Frequency Response Characteristics of Propellant Vaporization. NASA TN D-3749, 1966.

3. Bloomer, Henry E.; Wanhainen, John P.; and Vincent David W.: Chamber Shape Effects on Combustion Instability. Presented at Fourth ICRPG Combustion Conference, 1967.

4. Wanhainen, John P.; Parish, Harold C.; and Conrad, E. William: Effect of Propellant Injection Velocity on Screech in a 20,000-Pound Hydrogen-Oxygen Rocket Engine. NASA TN D-3373, 1966.

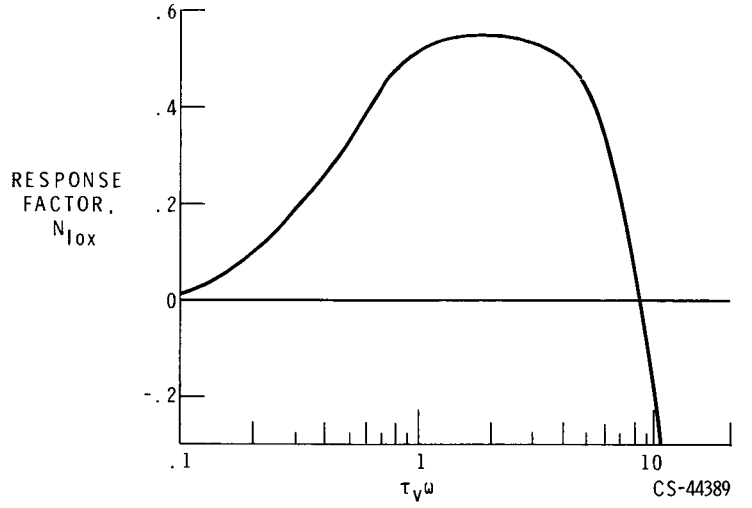

Figure 1. - Oxygen response factor.

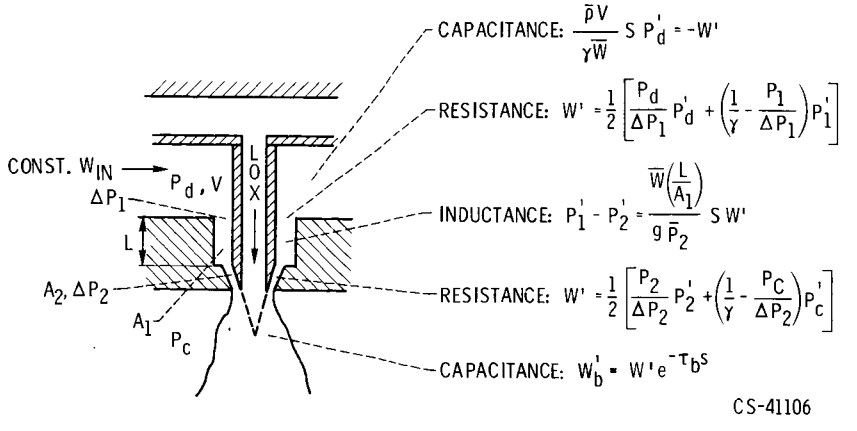

Figure 2. - Hydrogen model.

$$N_{H_2} = \left(\frac{W'_{b,max}}{P'_{c,max}}\right)\cos\theta$$

$$\frac{W'_{b,max}}{P'_{c,max}} = -\frac{\left(\frac{\bar{P}_c}{\Delta P_2} - \frac{1}{\gamma}\right)\left(\frac{\bar{P}_2}{\Delta P_1} - \frac{1}{\gamma}\right)\left(\frac{\Delta P_2}{\bar{P}_2}\right)\left(\frac{\Delta P_1}{\bar{P}_d}\right)C\omega}{\left(\left[1 - \frac{\Delta P_1}{\bar{P}_d}\left(\frac{\bar{P}_2}{\Delta P_1} - \frac{1}{\gamma}\right)CI\omega^2\right]^2 + \left\{2\frac{\Delta P_1}{\bar{P}_d}\left[1 + \frac{\Delta P_2}{\bar{P}_2}\left(\frac{\bar{P}_2}{\Delta P_1} - \frac{1}{\gamma}\right)\right]C\omega\right\}^2\right)^{1/2}}$$

$$\theta = \frac{\pi}{2} - \omega\tau_b - \tan^{-1}\frac{2\frac{\Delta P_1}{\bar{P}_d}\left[1 + \frac{\Delta P_2}{\bar{P}_2}\left(\frac{\bar{P}_2}{\Delta P_1} - \frac{1}{\gamma}\right)\right]C\omega}{1 - \frac{\Delta P_1}{\bar{P}_d}\left(\frac{\bar{P}_2}{\Delta P_1} - \frac{1}{\gamma}\right)CI\omega^2}$$

STABILITY CRITERION

$$\Sigma N = \frac{\bar{W}_t}{\bar{W}_t}N_{noz} + \frac{\bar{W}_{lox}}{\bar{W}_t}N_{lox} + \frac{\bar{W}_{H_2}}{\bar{W}_t}N_{H_2} = 0$$

CS-44326

Figure 3. - Response factor.

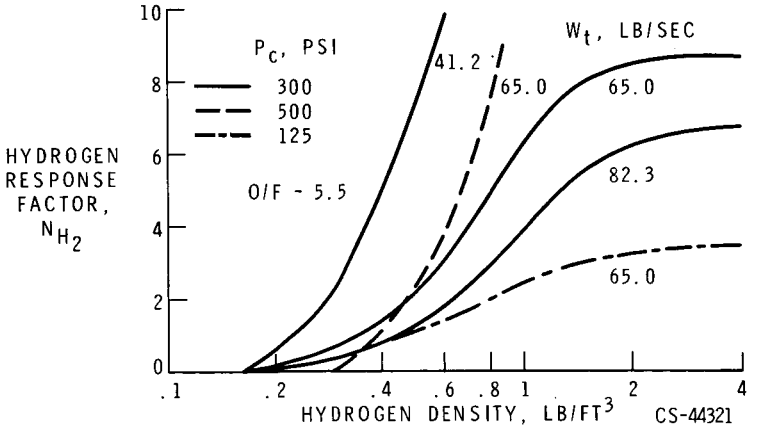

Figure 4. - Effect of flow rate and chamber pressure on response factor-density characteristics.

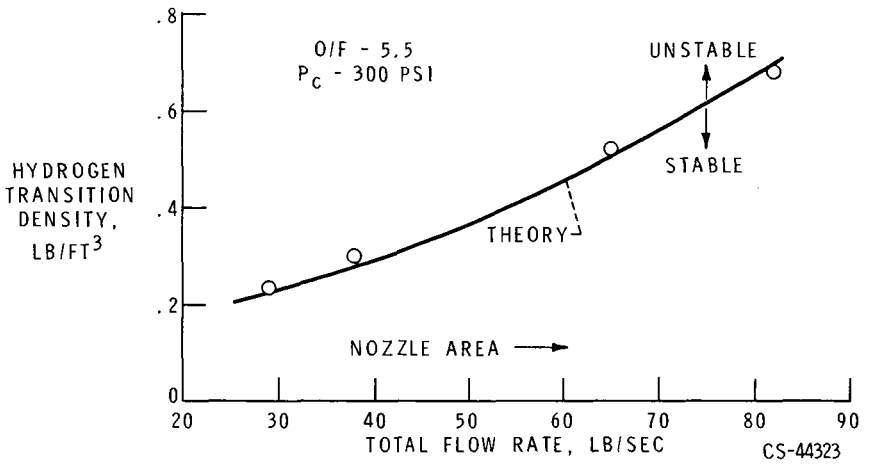

Figure 5. - Effect of flow rate on hydrogen transition density at constant chamber pressure.

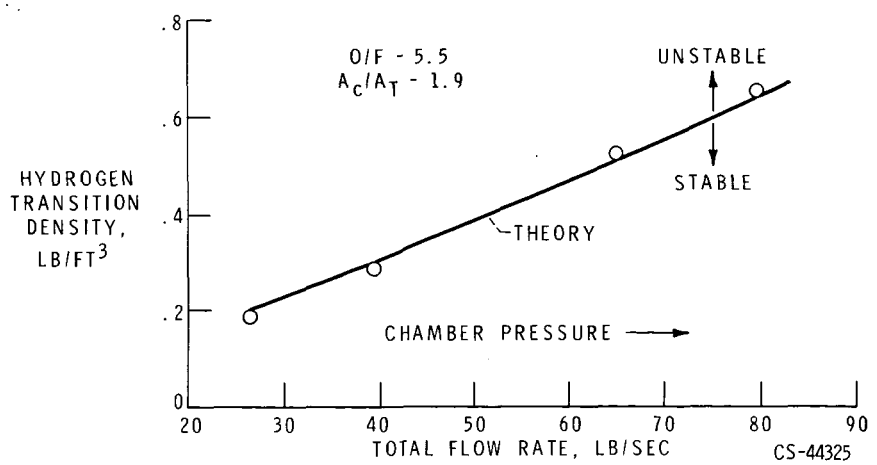

Figure 6. - Effect of flow rate on hydrogen transition density at constant contraction ratio.

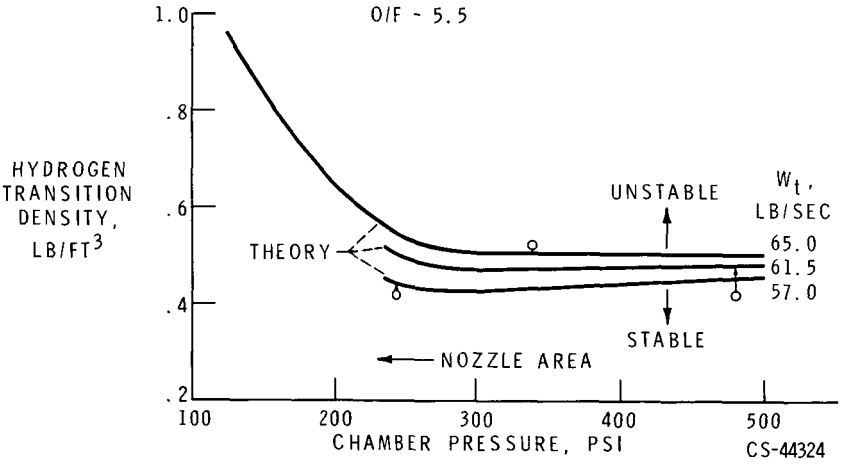

Figure 7. - Effect of chamber pressure on hydrogen transition density.

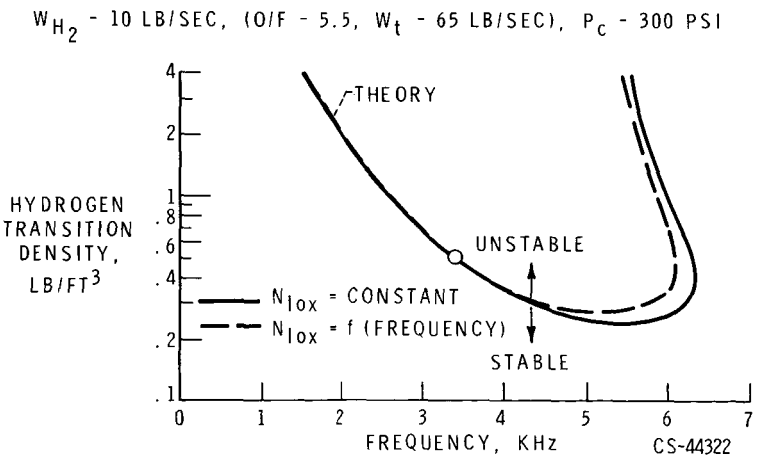

Figure 8. - Effect of frequency on hydrogen transition density for "standard" Lewis element.